3546 *Organometallics* **2010,** *29,* 3546–3555
DOI: 10.1021/om100424j

ORGANOMETALLICS
Article

Synthesis, Structure, and Insertion Reactivity of Zirconium and Hafnium Amidate Benzyl Complexes

Robert K. Thomson and Laurel L. Schafer*

Department of Chemistry, University of British Columbia, 2036 Main Mall, Vancouver, British Columbia, Canada, V6T 1Z3

Received May 5, 2010

A series of amidate-ligated dibenzyl zirconium and hafnium complexes are accessed through protonolysis reactions of the amide proligands 2,6-dimethylphenylpivaloylamide, $[^{\mathrm{DMP}}(\mathrm{NO})^{\mathrm{tBu}}]\mathrm{H}$ (**3**), and 1,3-bis(1-adamantylamide)-2,2-dimethylpropane, $^{\mathrm{Ad}}[\mathrm{O_2N_2}]\mathrm{H_2}$ (**5**), with $\mathrm{Zr(CH_2Ph)_4}$ or $\mathrm{Hf(CH_2Ph)_4}$. The resulting dibenzyl complexes $[^{\mathrm{DMP}}(\mathrm{NO})^{\mathrm{tBu}}]_2\mathrm{Zr(CH_2Ph)_2}$ (**4**), $^{\mathrm{Ad}}[\mathrm{O_2N_2}]\mathrm{Zr(CH_2Ph)_2(THF)}$ (**6**), and $^{\mathrm{Ad}}[\mathrm{O_2N_2}]\mathrm{Hf(CH_2Ph)_2(THF)}$ (**7**) are structurally characterized. Insertion reactions of **4** with isocyanides are investigated, resulting in the formation of an η^2-iminoacyl species, $[^{\mathrm{DMP}}(\mathrm{NO})^{\mathrm{tBu}}]_2\mathrm{Zr}(\eta^2\text{-}2,6\text{-}\mathrm{Me_2C_6H_3N{=}CCH_2Ph})_2$ (**8**), which undergoes thermal C=C coupling to form an enediamido complex, $[^{\mathrm{DMP}}(\mathrm{NO})^{\mathrm{tBu}}]_2\mathrm{Zr}(\eta^4\text{-}\mathrm{ArNC(CH_2Ph){=}C(CH_2Ph)NAr})$ (Ar = 2,6-$\mathrm{Me_2C_6H_3}$) (**9**). Analogous insertion of $^{\mathrm{t}}\mathrm{BuN{\equiv}C}$ into the Zr−C bonds of **4** results in the formation of a vinylamido complex, $[^{\mathrm{DMP}}(\mathrm{NO})^{\mathrm{tBu}}]_2\mathrm{Zr(N(^tBu)CH{=}CHPh)_2}$ (**10**), through a presumed 1,2-hydrogen migration mechanism from an iminoacyl intermediate similar to **8**. Complexes **8** and **9** are also structurally characterized.

Introduction

Selective C−C bond formation remains a challenging transformation for the rationally designed synthesis of targeted compounds and/or materials. Organometallic chemistry has played an extremely important role in the selective preparation of C−C bonds, due to the prevalence of transition metal−carbon bonded species as key intermediates in such transformations.[1] Our research group and others have been investigating amidate complexes of the group 4 metals for various catalytic applications.[2,3] Amidate complexes of a variety of metals have been prepared and fully characterized.[2−4] These amidate ligands can chelate hard early transition metals as σ-bonded four-electron donors. Thus, a hallmark of this class of complexes is the generation of very electropositive, sterically accessible metal centers. This is due to the nonsymmetric nature of amidate binding and the tight bite angles (approximately 60°) imposed by the four-membered metallacycle. Two closely related ligand systems to amidates are the amidinate[5] and guanidinate[6] ligands, which have been widely studied for a broad range of catalytic and stoichiometric organometallic transformations.

---

*To whom correspondence should be addressed. E-mail: schafer@chem.ubc.ca.

[1] Selected recent reviews include: (a) Colby, D. A.; Bergman, R. G.; Ellman, J. A. *Chem. Rev.* **2010**, *110*, 624–655. (b) Doyle, M. P.; Duffy, R.; Ratnikov, M.; Zhou, L. *Chem. Rev.* **2010**, *110*, 704–724. (c) Gunay, A.; Theopold, K. H. *Chem. Rev.* **2010**, *110*, 1060–1081. (d) Johansson, C. C. C.; Colacot, T. J. *Angew. Chem., Int. Ed.* **2010**, *49*, 676–707. (e) Ashenhurst, J. A. *Chem. Soc. Rev.* **2010**, *39*, 540–548.

[2] (a) Zhang, Z.; Schafer, L. L. *Org. Lett.* **2003**, *5*, 4733–4736. (b) Li, C.; Thomson, R. K.; Gillon, B.; Patrick, B. O.; Schafer, L. L. *Chem. Commun.* **2003**, 2462–2463. (c) Zhang, Z.; Leitch, D. C.; Lu, M.; Patrick, B. O.; Schafer, L. L. *Chem.—Eur. J.* **2007**, *13*, 2012–2022. (d) Wood, M. C.; Leitch, D. C.; Yeung, C. S.; Kozak, J. A.; Schafer, L. L. *Angew. Chem., Int. Ed.* **2007**, *46*, 354–358. (e) Thomson, R. K.; Bexrud, J. A.; Schafer, L. L. *Organometallics* **2006**, *25*, 4069–4071. (f) Ayinla, R. O.; Schafer, L. L. *Inorg. Chim. Acta* **2006**, *359*, 3097–3102. (g) Lee, A. V.; Schafer, L. L. *Synlett* **2006**, 2973–2976. (h) Lee, A. V.; Schafer, L. L. *Eur. J. Inorg. Chem.* **2007**, 2243–2255. (i) Bexrud, J. A.; Li, C.; Schafer, L. L. *Organometallics* **2007**, *26*, 6366–6372.

[3] (a) Kissounko, D. A.; Guzei, I. A.; Gellman, S. H.; Stahl, S. S. *Organometallics* **2005**, *24*, 5208–5210. (b) Kissounko, D. A.; Hoerter, J. M.; Guzei, I. A.; Cui, Q.; Gellman, S. H.; Stahl, S. S. *J. Am. Chem. Soc.* **2007**, *129*, 1776–1783. (c) Zi, G.; Liu, X.; Xiang, L.; Song, H. *Organometallics* **2009**, *28*, 1127–1137. (d) Zi, G.; Zhang, F.; Xiang, L.; Chen, Y.; Fang, W.; Song, H. *Dalton Trans.* **2010**, *39*, 4048–4061. (e) Gott, A. L.; Clarke, A. J.; Clarkson, G. J.; Scott, P. *Organometallics* **2007**, *26*, 1729–1737. (f) Liu, S.; Sun, W.-H.; Zeng, Y.; Wang, D.; Zhang, W.; Li, Y. *Organometallics* **2010**, *29*, 2459–2464. (g) Reznichenko, A. L.; Hultzsch, K. C. *Organometallics* **2010**, *29*, 24–27.

[4] (a) Fujita, K.; Yamashita, M.; Puschmann, F.; Alverez-Falcon, M. M.; Incarvito, C. D.; Hartwig, J. F. *J. Am. Chem. Soc.* **2006**, *128*, 9044–9045. (b) Jones, M. B.; Hardcastle, K. I.; MacBeth, C. E. *Polyhedron* **2009**, *29*, 116–119. (c) Jones, M. B.; Newell, B. S.; Hoffert, W. A.; Hardcastle, K. I.; Shores, M. P.; MacBeth, C. E. *Dalton Trans.* **2010**, *39*, 401–410.

[5] (a) Hagadorn, J. R.; Arnold, J. *Organometallics* **1994**, *13*, 4670–4672. (b) Stewart, P. J.; Blake, A. J.; Mountford, P. *Inorg. Chem.* **1997**, *36*, 3616–3622. (c) Littke, A.; Sleiman, N.; Bensimon, C.; Richeson, D. S.; Yap, G. P. A.; Brown, S. J. *Organometallics* **1998**, *17*, 446–451. (d) Stewart, P. J.; Blake, A. J.; Mountford, P. *J. Organomet. Chem.* **1998**, *564*, 209–214. (e) Stewart, P. J.; Blake, A. J.; Mountford, P. *Organometallics* **1998**, *17*, 3271–3281. (f) Keaton, R. J.; Koterwas, L. A.; Fettinger, J. C.; Sita, L. R. *J. Am. Chem. Soc.* **2002**, *124*, 5932–5933. (g) van Meerendonk, W. J.; Schroder, K.; Brussee, E. A. C.; Meetsma, A.; Hessen, B.; Teuben, J. H. *Eur. J. Inorg. Chem.* **2003**, 427–432. (h) Guiducci, A. E.; Boyd, C. L.; Mountford, P. *Organometallics* **2006**, *25*, 1167–1187.

[6] (a) Wood, D.; Yap, G. P. A.; Richeson, D. S. *Inorg. Chem.* **1999**, *38*, 5788–5794. (b) Mullins, S. M.; Duncan, A. P.; Bergman, R. G.; Arnold, J. *Inorg. Chem.* **2001**, *40*, 6952–6963. (c) Ong, T.-G.; Yap, G. P. A.; Richeson, D. S. *Chem. Commun.* **2003**, 2612–2613. (d) Ong, T.-G.; Yap, G. P. A.; Richeson, D. S. *Organometallics* **2003**, *22*, 387–389. (e) Bazinet, P.; Wood, D.; Yap, G. P. A.; Richeson, D. S. *Inorg. Chem.* **2003**, *42*, 6225–6229. (f) Duncan, A. P.; Mullins, S. M.; Arnold, J.; Bergman, R. G. *Organometallics* **2001**, *20*, 1808–1819.

More recently, ureate ligand systems have also shown complementary reactivity to the amidate-bound complexes.[7] Notably, stoichiometric insertion studies of C−E multiple bonds (E = N, O, S) into amidinate and guanidinate organometallic species have shown interesting reactivity profiles in comparison to those of other group 4 complexes.[5,6,8] These results on related ligand sets, coupled with our observations of unique catalytic activity that is accessible with amidate complexes,[2,3,9] suggest that complementary reactivity may be observed with amidate-supported group 4 organometallic complexes.

The synthesis of amidate-supported amido complexes and homoleptic amidate species via protonolysis with homoleptic titanium, zirconium, and yttrium amido starting materials is very facile and has been previously reported.[2h,3c,10−12] Furthermore, organometallic dibenzyl complexes of zirconium and hafnium can be synthesized through protonolysis using two equivalents of proligand, from easily prepared $M(CH_2Ph)_4$ starting materials (M = Zr, Hf).[13] Notably, amidate-supported titanium and zirconium benzyl complexes have been prepared by Scott and co-workers using this protonolysis approach.[3e]

We communicated the first group 4 amidate alkyl complexes **1** and **2**, which are prepared via protonolysis using two equivalents of the proligand 2,6-dimethyphenylbenzamide ([$^{\mathrm{DMP}}$(NO)$^{\mathrm{Ph}}$]H) and $Hf(CH_2Ph)_4$.[14] While the THF adduct **1** has been structurally characterized, the unsolvated species **2** (eq 1) could be observed in the solution phase, but could be obtained only as an amorphous powder in the solid state.[14]

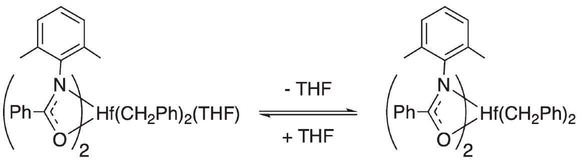

(1)

1, *Orange* **2**, *Yellow*

Building upon these preliminary results, here we discuss the synthesis and characterization of new organometallic zirconium and hafnium amidate complexes and their subsequent insertion reactivity with alkyl and aryl isocyanides, which leads to both rearrangement and C−C coupling reactions.

Results and Discussion

Synthesis and Characterization of Dibenzyl Complexes. Complex **1** has been fully characterized, and this seven-coordinate pseudo-pentagonal bipyramidal species has the amidate ligands in the equatorial plane.[14] Interestingly, an unusual and sterically unfavorable *cis*-N geometry of the amidate ligands is observed in the solid-state molecular structure, presumably due to stabilization by π-stacking interactions between the 2,6-dimethylphenyl units of the amidate ligands. In complex **1**, the benzyl ligands are arranged in a *trans* fashion, in contrast to previously characterized seven-coordinate amidate-supported bis(amido) complexes, which have the amido ligands *cis* to each other.[2d] As described above, the coordinated THF ligand is labile in solution, as observed by ^1H NMR spectroscopy, resulting in an equilibrium with the unsolvated species **2** (eq 1). This complex displays solvatochromic behavior and changes from an orange solution to a yellow solution upon removal of the THF solvent under vacuum.[14]

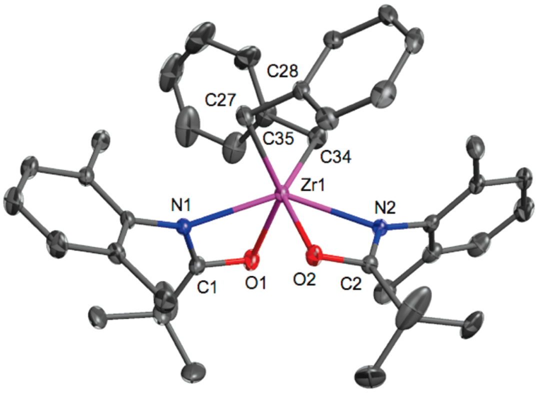

Figure 1. ORTEP depiction of the solid-state molecular structure of $[^{DMP}(NO)^{tBu}]_2Zr(CH_2Ph)_2$, **4** (ellipsoids at 30% probability, hydrogens omitted).

While solid-state molecular structural analysis of the six-coordinate hafnium complex **2** was not possible, the proposed structure, based upon solution phase behavior, is a pseudo-octahedral species with a *cis* arrangement of the benzyl ligands, exhibiting overall C_2 symmetry. Such a C_2 symmetric structure can be characterized in the solid state for the related six-coordinate zirconium dibenzyl complex $[^{DMP}(NO)^{tBu}]_2Zr(CH_2Ph)_2$ (**4**, Figure 1). This compound is synthesized in 80% yield using the synthetic protocol presented in eq 2.

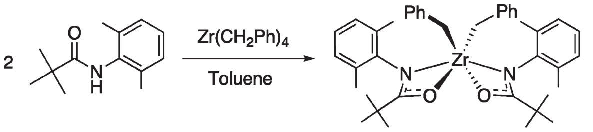

(2)

3 **4**

Dibenzyl complex **4** is isolated as a bright yellow powder and can be readily recrystallized from pentane. The solid-state molecular structure is shown in Figure 1. Selected bond lengths and angles are collected in Table 1, and crystallographic data in Table 2. Solution phase behavior of **4** is consistent with C_2 symmetry, as indicated by single resonances for the amidate *tert*-butyl and aryl methyl groups at δ 0.91 and 2.05, respectively. This suggests free rotation about the $N-C_{ipso}$ bonds of the 2,6-dimethylphenyl substituents. Free rotation of the benzyl groups is also observed by a single resonance at δ 2.24. Variable-temperature ^1H NMR experiments on **4** do not indicate any slow fluxional processes that can be arrested at low temperature (spectra were recorded as low as −80 °C). It is important to note that even when THF is used as the reaction solvent, **4** does not form a seven-coordinate

---

(7) (a) Leitch, D. C.; Beard, J. D.; Thomson, R. K.; Wright, V. A.; Patrick, B. O.; Schafer, L. L. *Eur. J. Inorg. Chem.* **2009**, 2691–2701. (b) Leitch, D. C.; Dunbar, C. R.; Payne, P. R.; Schafer, L. L. *J. Am. Chem. Soc.* **2009**, *131*, 18246–18247.

(8) Ong, T.-G.; Wood, D.; Yap, G. P. A.; Richeson, D. S. *Organometallics* **2002**, *21*, 1–3.

(9) Bexrud, J. A.; Eisenberger, P.; Leitch, D. C.; Payne, P. R.; Schafer, L. L. *J. Am. Chem. Soc.* **2009**, *131*, 2116–2118.

(10) Bexrud, J. A.; Schafer, L. L. *Dalton Trans.* **2010**, *39*, 361–363.

(11) Stanlake, L. J. E.; Beard, J. D.; Schafer, L. L. *Inorg. Chem.* **2008**, *47*, 8062–8068.

(12) Thomson, R. K.; Zahariev, F. E.; Zhang, Z.; Patrick, B. O.; Wang, Y. A.; Schafer, L. L. *Inorg. Chem.* **2005**, *44*, 8680–8689.

(13) Zucchini, U.; Albizzati, E.; Giannini, U. *J. Organomet. Chem.* **1971**, *26*, 357–372.

(14) Thomson, R. K.; Patrick, B. O.; Schafer, L. L. *Can. J. Chem.* **2005**, *83*, 1037–1042.

Table 1. Selected Bond Lengths (Å) and Angles (deg) for Dibenzyl Complexes 4, 6, and 7

4		6		7	
Zr1−O1	2.099(1)	Zr1−O1	2.208(2)	Hf1−O1	2.193(2)
Zr1−O2	2.108(1)	Zr1−O2	2.196(2)	Hf1−O2	2.181(2)
Zr1−N1	2.284(1)	Zr1−O3	2.289(2)	Hf1−O3	2.256(2)
Zr1−N2	2.288(1)	Zr1−N1	2.183(2)	Hf1−N1	2.166(2)
Zr1−C27	2.244(2)	Zr1−N2	2.187(2)	Hf1−N2	2.174(2)
Zr1−C34	2.239(2)	Zr1−C28	2.358(3)	Hf1−C28	2.341(4)
O1−Zr1−O2	95.75(5)	Zr1−C35	2.366(3)	Hf1−C35	2.357(4)
N1−Zr1−N2	142.16(5)	O1−Zr1−O2	161.62(7)	O1−Hf1−O2	160.35(8)
N1−Zr1−C27	82.98(6)	O1−Zr1−O3	82.46(6)	O1−Hf1−O3	81.68(8)
O1−Zr1−C27	139.85(5)	O2−Zr1−O3	81.29(6)	O2−Hf1−O3	81.14(8)
C27−Zr1−C34	97.18(8)	O2−Zr1−N2	59.84(7)	O2−Hf1−N2	60.28(9)
C28−C27−Zr1	103.8(1)	O1−Zr1−N1	59.68(7)	O1−Hf1−N1	60.00(9)
C35−C34−Zr1	105.1(1)	N2−Zr1−N1	77.74(7)	N2−Hf1−N1	78.13(9)
O1−Zr1−N1	58.78(5)	C28−Zr1−C35	165.6(1)	C28−Hf1−C35	168.7(1)
O1−C1−N1	112.55(1)	C29−C28−Zr1	113.5(2)	C29−C28−Hf1	115.1(2)
		C36−C35−Zr1	116.6(2)	C36−C35−Hf1	114.2(2)
		O1−C1−N1	113.2(2)	O1−C1−N1	112.2(3)

Table 2. Crystallographic Data for Complexes 4, 6, 7, 8, and 9

	4	6	7	8	9
empirical formula	$C_{40}H_{50}N_2O_2Zr$	$C_{45}H_{62}N_2O_3Zr$	$C_{45}H_{62}N_2O_3Hf$	$C_{58}H_{68}N_4O_2Zr$	$C_{58}H_{68}N_4O_2Zr$
fw	682.04	770.19	857.46	944.38	944.38
cryst syst	triclinic	triclinic	triclinic	monoclinic	monoclinic
space group	$P\bar{1}$ (#2)	$P\bar{1}$ (#2)	$P\bar{1}$ (#2)	$P2_1/c$	$P2_1/n$
a (Å)	9.719(2)	8.8174(7)	11.4687(12)	19.475(5)	13.036(4)
b (Å)	12.169(3)	11.5483(9)	17.4135(18)	12.736(5)	22.774(7)
c (Å)	16.612(4)	21.155(3)	22.171(2)	20.838(5)	16.957(5)
α (deg)	72.624(10)	86.984(10)	103.5860(10)	90	90
β (deg)	85.866(11)	82.894(9)	94.322(2)	90.379(5)	94.825(10)
γ (deg)	76.118(10)	69.810(6)	109.066(3)	90	90
V (Å^3)	1820.3(7)	2006.2(3)	4011.6(7)	5168(3)	5016(3)
Z	2	2	4	4	4
D_c (g·cm^{-3})	1.244	1.275	1.420	1.214	1.250
T (K)	173 ± 1	173 ± 1	173 ± 1	173 ± 1	173 ± 1
solvent/color	pentane/yellow	hexanes/yellow	hexanes/yellow	pentane/colorless	toluene/yellow
(h, k, l)	$-16 \leq h \leq 14$ $-19 \leq k \leq 17$ $-26 \leq l \leq 24$	$-11 \leq h \leq 11$ $-15 \leq k \leq 15$ $-26 \leq l \leq 27$	$-14 \leq h \leq 12$ $-22 \leq k \leq 22$ $-27 \leq l \leq 26$	$-20 \leq h \leq 20$ $-13 \leq k \leq 13$ $-22 \leq l \leq 18$	$-18 \leq h \leq 18$ $-31 \leq k \leq 31$ $-23 \leq l \leq 23$
F(000)	720	820	1768	2000	2000
θ range (deg)	1.28−36.55	2.11−27.88	2.27−27.88	2.14−22.65	1.50−30.27
linear abs coeff (mm^{-1})	0.337	0.315	0.264	0.257	0.265
total no. of reflns collected	52 902	17 662	35 599	48 486	64 748
no. of unique reflns ($F > 4\sigma(F)$)	11 233	7282	13 738	4552	9945
no. of obsd reflns	15 411	8114	16 302	6785	14 747
R_{int}	0.0458	0.0461	0.0407	0.0708	0.0645
R_1, wR_2 ($I > 2\sigma(I)$)	0.0707, 0.1359	0.0494, 0.1127	0.0368, 0.0749	0.1215, 0.2504	0.0888, 0.1549
GoF	1.044	1.087	1.068	1.055	1.033
peak/hole (e/Å^3)	0.610, −0.515	1.009, −1.023	1.614, −1.557	2.337, −1.216	0.647, −0.901

complex analogous to **1**. In comparison to the hafnium complex **1**, **4** is significantly more photochemically and thermally prone to degradation.

The structure of **4** is C_2 symmetric, with the nitrogen donors of the amidate ligands *trans* to each other. While η^1-coordination of the benzyl group is obvious for **1**,[14] the hapticity of the benzyl group in **4** is less clear. The typical parameters used to evaluate the hapticity of benzyl ligands are (1) the bond angle formed by the *ipso* carbon of the benzyl group, the benzylic carbon, and the metal center,[15] (2) the chemical shift of the *ortho* protons of the benzyl group,[16] and (3) the sum of the van der Waals radii of the metal center and the *ipso* carbon.[17] In this case, the bond angles at the benzylic carbon atoms in **4** are 103.8(1)° and 105.1(1)° and are considerably more acute than the 122.3(4)° and 124.3(4)° bond angles for **1**, but still obtuse compared to previously observed angles near 90°.[16b,17b,18] While a wide variation in this bond angle has been observed to be dependent upon the steric and electronic requirements of the metal center,[19] the bond angles in **4** are best classified as intermediate between η^1- and η^2-hapticity for the benzyl group.[16a] A similar "intermediate" hapticity has been reported for a β-diketiminate tribenzyl species, (TTP)Zr(CH_2Ph)$_3$ (TTP = *p*-tolyl-NC(CH_3)CHC(CH_3)N-*p*-tolyl),[20] and the Cp complex

---

(15) Dryden, N. H.; Legzdins, P.; Trotter, J.; Yee, V. C. *Organometallics* **1991**, *10*, 2857–2870.

(16) (a) Latesky, S. L.; McMullen, A. K.; Niccolai, G. P.; Rothwell, I. P.; Huffman, J. C. *Organometallics* **1985**, *4*, 902–908. (b) Dryden, N. H.; Legzdins, P.; Phillips, E. C.; Trotter, J.; Yee, V. C. *Organometallics* **1990**, *9*, 882–884.

(17) (a) Cotton, F. A.; Wilkinson, G.; Murillo, C. A.; Bochmann, M. *Advanced Inorganic Chemistry*, 6th ed.; John Wiley & Sons, Inc.: Toronto, 1999. (b) Legzdins, P.; Phillips, E. C.; Trotter, J.; Yee, V. C.; Einstein, F. W. B.; Jones, R. H. *Organometallics* **1991**, *10*, 986–1002.

(18) Warren, T. H.; Schrock, R. R.; Davis, W. M. *Organometallics* **1996**, *15*, 562–569.

(19) Carmona, E.; Marin, J. M.; Paneque, M.; Poveda, M. L. *Organometallics* **1987**, *6*, 1757–1765.

(20) Qian, B.; Scanlon, W. J.; Smith, M. R. *Organometallics* **1999**, *18*, 1693–1698.

$CpZr(CH_2Ph)_3$, which has a benzyl ligand with a bond angle of 94.5°.[21]

Given the acute angles formed at the benzylic carbon atoms and the overall C_2 symmetry of **4**, it is surprising that the diastereotopic benzylic protons do not manifest as two different signals. Fluxional processes are likely responsible for this observation. Interconversion between η^1- and η^2-coordination modes of the benzyl ligands is possible; however, variable-temperature ^1H NMR experiments do not indicate any observable changes at low temperature. With η^2-benzyl ligands, it is often seen that the *ortho* protons are shifted to higher field, which can be attributed to significant π-donation to the metal center.[16a] For **4**, no arene resonances are observed upfield of approximately δ 6.8, which is generally considered the cutoff for η^2-behavior,[16a] supporting average η^1-binding in the solution phase. It is also possible that the amidate ligands undergo isomerization in solution through a κ^1-O-bound amidate intermediate that cannot be observed, even when using low-temperature ^1H NMR spectroscopic experiments. However, this isomerization process seems less probable for these dibenzyl complexes, as the benzyl ligands offer less electronic stabilization than the amido ligands in the bis(amidate) bis(amido) complexes reported previously.[12]

Inspection of the distances between Zr1 and the *ipso* carbon atoms (C28−2.97 Å and C35−2.98 Å) shows that they fall well outside the distance expected for formal Zr−C bonds, which are usually approximately 2.2−2.4 Å.[16a,22] However, weak noncovalent interactions between zirconium and the *ipso* benzyl carbons are present, since the Zr1−C28 and Zr1−C35 distances fall within the sum of the van der Waals radii of Zr and C (~3.7 Å).[23] These data taken together suggest a degree of η^2-character for the benzyl ligands in **4** in the solid state, which may be due to crystal packing, especially considering that, in the solution phase, data are indicative of η^1-hapticity.

Tethered Tetradentate Amidate Dibenzyl Complexes. In contrast to the titanium bis(amidate) bis(amido) complexes described previously, the dibenzyl complexes **1**, **2**, and **4** do not appear to undergo amidate ligand isomerization as readily.[12] This reduces the need for a tethered bis(amidate) ligand to control geometric isomerization. However, the ability to access a *trans*-type pentagonal bipyramidal geometry for the hafnium dibenzyl complex **1** indicates that the tethered proligand 1,3-bis(1-adamantylamide)-2,2-dimethylpropane, $^{Ad}[O_2N_2]H_2$ (**5**), should be suitable for stabilizing bis(alkyl) complexes of zirconium and hafnium, as this ligand should preferentially bind in a planar fashion.[2d,7a] Synthesis of the zirconium (**6**) and hafnium (**7**) dibenzyl complexes of proligand **5** can be accomplished as shown in eq 3.

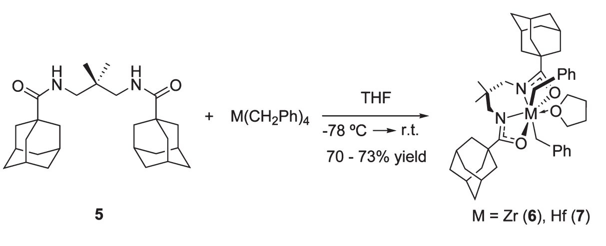

(3)

5

M = Zr (**6**), Hf (**7**)

While this reaction is completely analogous to the synthesis of **1**, **2**, and **4**, additional care must be taken when performing these protonolysis reactions with proligand **5**. The extra entropic driving force provided by the chelate effect of the tetradentate ligand set can result in the formation of homoleptic species as byproducts in these reactions, even when performed in a strict 1:1 stoichiometry. The extremely low solubility of **5** in nearly all common solvents makes the slow addition of a solution of **5** to a solution of $M(CH_2Ph)_4$ unfeasible, and addition of cold solvent to an intimate mixture of **5** and $M(CH_2Ph)_4$ still results in the formation of large quantities of homoleptic byproducts. To circumvent this problem, the slow addition of **5** to a THF solution of $M(CH_2Ph)_4$ via solid addition funnel is required. This results in high yields of the desired dibenzyl species as bright yellow ($^{Ad}[O_2N_2]Zr(CH_2Ph)_2(THF)$, **6**) and pale yellow ($^{Ad}[O_2N_2]Hf(CH_2Ph)_2(THF)$, **7**) powders.

As illustrated in eq 3, these complexes are stabilized by THF in solution, with signals for coordinated THF appearing at δ 1.33 and 3.99 for **7**. The ^1H NMR spectra for **6** and **7** are nearly identical, suggesting that they are isostructural. Solution phase C_{2v} geometry is supported by the high symmetry of the ^1H NMR spectra of **6** and **7**, with a single resonance observed for the amidate ligand tether methyl groups of **7** at δ 0.86, suggesting a tether ring-flipping process on the NMR time scale. Likewise, single resonances for the benzylic and tether methylene protons are observed at δ 1.73 and 3.19, respectively. The protons of the bulky adamantyl groups appear as three resonances in a 2:1:2 ratio at δ 1.66, 1.95, and 2.09.

Similar to complexes **1**, **2**, and **4**, complexes **6** and **7** do not exhibit any solution behavior suggestive of η^2-coordination of the benzyl groups. Free rotation of the benzyl groups about their M−C bonds in solution is facile and cannot be arrested during low-temperature ^1H NMR experiments. Interestingly, unlike **1**, the coordinated THF ligand in **6** and **7** is not labile in solution. Since these THF adducts are formally 14-electron species, the coordination of THF helps satisfy the electronic requirements of the metal centers in these species. The lack of THF lability may be due to the fact that this tethered bis(amidate) ligand does not offer sufficient flexibility to assume a more traditional pseudo-octahedral geometry upon loss of THF. Verification of the planar binding geometry of the bis(amidate) ligand in complexes **6** and **7** is given in their solid-state molecular structures in Figure 2, with selected bond lengths and angles presented in Table 1.

The metrical parameters given in Table 1 are unexceptional and show that **6** demonstrates very similar bond lengths and angles to **1** and **4**, where the amidate unit bite angle in all of these complexes is approximately 60°. The bond angle between the *trans* benzyl groups is 165.6(1)°, which is slightly contracted in comparison to **1**, where this angle is 169.8(2)°.[14] The highly exposed nature of the zirconium center in **6** is apparent in Figure 2, where the bulky adamantyl groups effectively shield the metal center from the sides, but leave the metal center accessible from the top, bottom, and front. As observed previously for **1**, the THF coordinates in the equatorial position between the two benzyl groups, generating a pentagonal bipyramidal structure. The bond angles at the benzylic carbon atoms are obtuse, indicating η^1-binding of the benzyl ligands to Zr (C(29)−C(28)−Zr(1) = 113.5(2)° and C(36)−C(35)−Zr(1) = 116.6(2)°). The overall symmetry of **6** is C_s; however, rapid ring-flipping of the amidate tether and free rotation of the

---

[21] Scholz, J.; Rehbaum, F.; Thiele, K.-H.; Goddard, R.; Betz, P.; Krueger, C. *J. Organomet. Chem.* **1993**, *443*, 93–99.

[22] Jordan, R. F.; LaPointe, R. E.; Bajgur, C. S.; Echols, S. F.; Willett, R. *J. Am. Chem. Soc.* **1987**, *109*, 4111–4113.

[23] Bondi, A. *J. Phys. Chem.* **1964**, *68*, 441–451.

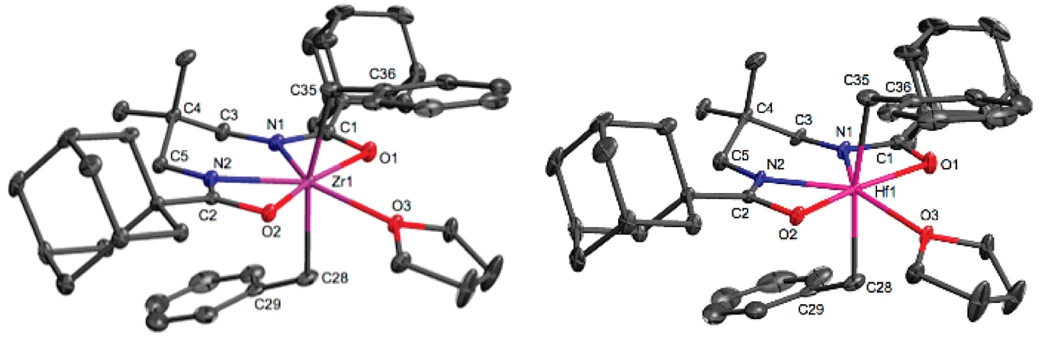

6 **7**

Figure 2. ORTEP depictions of solid-state molecular structures of $^{Ad}[O_2N_2]M(CH_2Ph)_2(THF)$, M = Zr (**6**), Hf (**7**) (ellipsoids at 30% probability).

benzyl groups about the Zr–C linkages give rise to the observed C_{2v} solution phase structure.

Single crystals of the hafnium congener **7** were also grown from pentane (Figure 2). Aside from a slight contraction of the bond distances between the ligand donor atoms and the metal center, **7** is completely isostructural to **6**. These bond length reductions can be attributed to hafnium relativistic effects, giving rise to slightly decreased bond lengths in the 5d congener when compared to the 4d complex.[17a]

Insertion Reactions of Isocyanides. Insertion of isocyanides into metal–carbon bonds is a well-known process that has been extensively studied; therefore, it is an attractive place to begin fundamental investigations of amidate-supported group 4 organometallic species.[24] The insertion of isocyanides into group 4 metal–carbon bonds is known to proceed through initial coordination of the carbon lone pair, followed by rapid insertion into the adjacent M–C bond.[24,25] This results in the formation of an iminoacyl complex, where the N=C bond is usually coordinated to the metal center in an η^2-fashion.[26] Unlike the reversible insertion of CO to form acyl species, the formation of iminoacyl complexes is irreversible, resulting in complexes that are stable to thermally induced deinsertion processes.[24]

The insertion of 2,6-dimethylphenyl isocyanide was investigated with zirconium dibenzyl complex **4**. Upon addition of two equivalents of isocyanide to a solution of **4** in C_6D_6 in a J-Young NMR tube, the solution is observed to immediately change from bright yellow to colorless. The ^{1}H NMR spectrum of the reaction mixture indicates formation of a single product in quantitative yield; however on a preparative scale the white powdery material can be isolated only in 52% yield. Successful insertion of the isocyanide moieties is suggested by the appearance of doublets at δ 3.35 and 3.59 corresponding to diastereotopic benzylic protons. The bis(iminoacyl) complex **8** ($[^{DMP}(NO)^{tBu}]_2Zr(\eta^2\text{-}2,6\text{-}Me_2C_6H_3N{=}CCH_2Ph)_2$) is nonfluxional in solution, where the presence of four singlets of equal intensity at δ 0.95, 1.92, 2.12, and 2.62 is suggestive of two unique 2,6-dimethylphenyl groups, each experiencing hindered rotation about the N–C_{ipso} bond. This is possible in a C_2 symmetric species, where the amidate ligand aryl groups and the inserted isocyanide aryl groups experience hindered rotation on the NMR time scale. Also, the notable upfield chemical shift of δ 0.95 for an aryl methyl substituent may be due to significant arene ring current induced deshielding from the adjacent group. Thus, on the basis of these spectroscopic data the insertion product **8** is proposed to have the structure shown in eq 4.

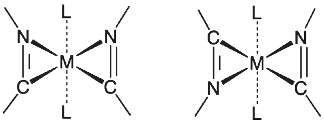

A **B**

Figure 3. Common geometric isomers of bis(η^2-iminoacyl) complexes.

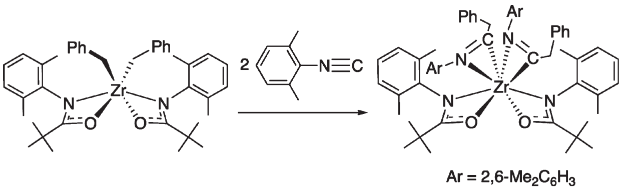

(4)

4 **8**

The η^2-binding mode in eq 4 is also suggested by ^{13}C NMR spectroscopic data, where the resonance at δ 250.6 is characteristic of η^2-coordinated iminoacyl carbons.[24,25] The most commonly observed geometric isomers of bis η^2-iminoacyls are best described as pseudo-tetrahedral in either a head-to-head (**A**) or head-to-tail (**B**) arrangement, as shown in Figure 3.[24,26b] Interconversion between these two forms can occur, and in some cases has been observed spectroscopically.[26d] The solution phase structure of **8** appears static at room temperature, as observed by ^{1}H NMR spectroscopy. Due to the observed C_2 symmetry, **8** is consistent with geometric isomer **B**, where the ancillary ligands (L) are κ^2-amidate groups. Variable-temperature ^{1}H NMR experiments suggest that interconversion between forms **A** and **B** is not particularly facile, as no change in the spectrum is observed over the range of temperatures (−40 to 90 °C).

The solid-state molecular structure of **8** is shown in Figure 4. Selected bond distances and angles are presented in Table 3. The presence of η^2-ligation is confirmed by Zr–N and Zr–C bond lengths that are nearly identical for each of the iminoacyl groups (Zr1–N3 = 2.243(6) Å, Zr1–C3 = 2.252(7) Å

---

(24) Durfee, L. D.; Rothwell, I. P. *Chem. Rev.* **1988**, *88*, 1059–1079.

(25) Scott, M. J.; Lippard, S. J. *Organometallics* **1997**, *16*, 5857–5868.

(26) (a) Spencer, L. P.; Fryzuk, M. D. *J. Organomet. Chem.* **2005**, *690*, 5788–5803. (b) Chamberlain, L. R.; Durfee, L. D.; Fanwick, P. E.; Kobriger, L.; Latesky, S. L.; McMullen, A. K.; Rothwell, I. P.; Folting, K.; Huffman, J. C. *J. Am. Chem. Soc.* **1987**, *109*, 390–402. (c) Giannini, L.; Caselli, A.; Solari, E.; Floriani, C.; Chiesi-Villa, A.; Rizzoli, C.; Re, N.; Sgamellotti, A. *J. Am. Chem. Soc.* **1997**, *119*, 9198–9210. (d) Thorn, M. G.; Lee, J.; Fanwick, P. E.; Rothwell, I. P. *J. Chem. Soc., Dalton Trans.* **2002**, 3398–3405. (e) Sebastian, A.; Royo, P.; Gomez-Sal, P.; Ramirez de Arellano, C. *Eur. J. Inorg. Chem.* **2004**, 3814–3821.

and Zr1−N4 = 2.246(6) Å, Zr1−C4 = 2.249(8) Å). As expected, the iminoacyl N=C bond lengths are consistent with double bonds (C3−N3 = 1.27(1) Å and C4−N4 = 1.282(9) Å), matching the structure shown in eq 4.[27] The head-to-tail arrangement of the iminoacyl ligands is also verified in the solid state, where the overall structure matches that for isomer **B** from Figure 3. In many cases where two η^2-iminoacyl ligands are bound to a group 4 metal, the L−M−L plane is not parallel to the iminoacyl N=C bonds and is twisted substantially from the C→N vectors (Figure 3).[24,26b] In the solid-state structure of **8**, the twist angle between the iminoacyl C→N vectors and the plane defined by C1−Zr1−C2 is approximately 26°, thereby allowing the bulky amidate N-substituents to be spatially removed from the bulky iminoacyl substituents. This is more easily viewed in Figure 4B, which shows **8** as viewed down its C_2 axis of symmetry. This twist angle is similar to the value seen for the bulky bis(aryloxy) zirconium complex (Zr(O-2,6-^{t}Bu$_2$C$_6$H$_3$)$_2$(η^2-^{t}BuN=CCH$_2$Ph)$_2$), which exhibits a twist angle of 21.5°.[26b]

While **8** is stable in solution at room temperature, heating this complex to 110 °C for 24 h results in the formation of a new bright yellow species having C_s symmetry in solution. ^{1}H NMR spectroscopy of the product of this reaction shows the presence of two resonances for the aryl methyl groups, indicating free rotation about the N−C$_{ipso}$ bonds of the 2,6-dimethylphenyl groups of the inserted isocyanides and the amidate ligands. Additionally, the ^{13}C NMR spectroscopic signal at δ 250.6 is absent, while a new signal at δ 115.6 is observed, indicative of an sp^2-hybridized carbon center. These results are consistent with a well-established coupling transformation (eq 5).[24,25,28]

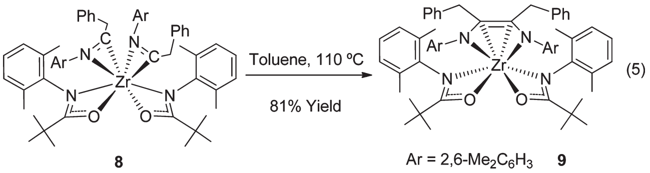

(5)

The formation of new C−C bonds by the coupling of isocyanides in the presence of early transition metals is dependent upon the steric and electronic properties of both the metal center and the isocyanides.[24] This process is generally intramolecular in nature and is dictated largely by the energy of the π^*_{CN} orbital.[29] Furthermore, coupling in this case is possible only if the iminoacyl ligands rearrange to the "head-to-head isomer A (Figure 3). Accordingly, C−C coupling is more readily achieved with electron-withdrawing groups on the iminoacyl moiety, such as aryl substituents, and less readily achieved with electron-donating alkyl groups on the iminoacyl unit.[29] The xylyl groups in **8** are slightly activating and, thus, fit this pattern of reactivity. Formation of a new C=C bond to generate the enediamido complex [^{DMP}(NO)^{tBu}]$_2$Zr(η^4-ArNC(CH$_2$Ph)=C(CH$_2$Ph)NAr), **9** (Ar = 2,6-Me$_2$C$_6$H$_3$), is confirmed by the solid-state molecular structure illustrated in Figure 5, with relevant bond lengths and angles given in Table 3.

Figure 5 shows that **9** is not C_s symmetric in the solid state, indicating that solution fluxionality must be occurring to

Table 3. Selected Bond Lengths (Å) and Angles (deg) for Insertion Products 8 and 9

8		**9**	
Zr1−O1	2.214(5)	Zr1−O1	2.134(2)
Zr1−O2	2.217(5)	Zr1−O2	2.164(2)
Zr1−N1	2.339(6)	Zr1−N1	2.470(2)
Zr1−N2	2.335(6)	Zr1−N2	2.346(2)
Zr1−N3	2.243(6)	Zr1−N3	2.033(2)
Zr1−N4	2.246(6)	Zr1−N4	2.069(2)
Zr1−C3	2.252(7)	Zr1−C27	2.560(2)
Zr1−C4	2.249(8)	Zr1−C28	2.548(2)
N3−C3	1.27(1)	C27−C28	1.381(3)
N4−C4	1.282(9)	N3−C28	1.406(3)
O1−Zr1−O2	79.3(2)	N4−C27	1.410(3)
N1−Zr1−N2	129.2(2)	O1−Zr1−N1	56.04(7)
C3−Zr1−C4	110.2(3)	O2−Zr1−N2	57.69(7)
N3−Zr1−N4	108.0(2)	C37−N3−Zr1	142.2(2)
N3−Zr1−C3	32.9(2)	C37−N3−C28	121.0(2)
N4−Zr1−C4	33.2(2)	C28−N3−Zr1	93.8(1)
C29−N3−C3	127.3(6)	C52−C28−N3	117.1(2)
C29−N3−Zr1	158.0(5)	C52−C28−C27	123.4(2)
C3−N3−Zr1	73.9(4)	C27−C28−N3	118.9(2)
C37−C3−Zr1	162.2(6)	C29−N4−Zr1	146.0(2)
C37−C3−N3	123.2(7)	C29−N4−C27	120.7(2)
N3−C3−Zr1	73.1(4)	C27−N4−Zr1	92.8(1)
C52−C4−Zr1	161.0(4)	C45−C27−N4	117.5(2)
C52−C4−N4	124.4(7)	C45−C27−C28	123.8(2)
N4−C4−Zr1	73.3(4)	C28−C27−N4	118.6(2)
C4−N4−Zr1	73.5(4)	O1−Zr1−O2	116.11(7)
C44−N4−C4	125.6(6)	N1−Zr1−N2	93.72(7)
C44−N4−Zr1	159.8(5)		

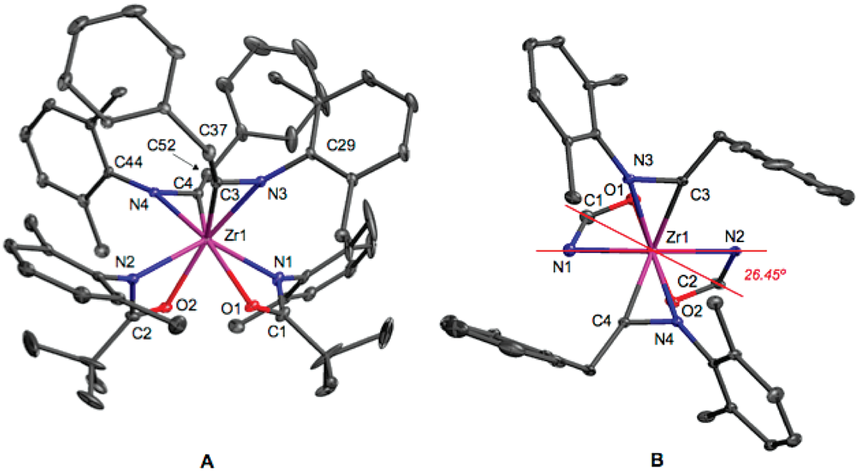

Figure 4. (A) ORTEP depiction (ellipsoids at 30% probability) of solid-state molecular structure of [^{DMP}(NO)^{tBu}]$_2$Zr(η^2-2,6-Me$_2$C$_6$H$_3$N=CCH$_2$Ph)$_2$, **8** (hydrogens omitted), (B) viewed down the C_2 axis of symmetry (amidate substituents and hydrogens omitted).

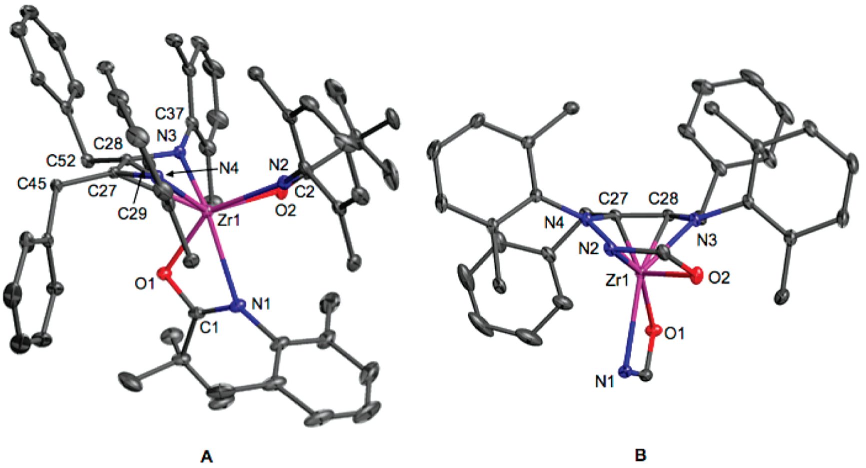

Figure 5. ORTEP depiction (ellipsoids at 30% probability) of $[^{DMP}(NO)^{tBu}]_2Zr(\eta^4\text{-}ArNC(CH_2Ph){=}C(CH_2Ph)NAr)$, **9** (Ar = 2,6-$Me_2C_6H_3$): (A) hydrogens omitted; (B) hydrogens and amidate substituents omitted.

give rise to the observed ^1H NMR spectrum. Solution phase amidate fluxionality has been observed previously, and a proposed $\kappa^2-\kappa^1-\kappa^2$ mechanism for this process must be considered.[12] The new C−C bond formed falls within the range expected for a double bond (C27−C28 = 1.381(3) Å), and the C−N distances of the enediamido backbone are consistent with single bonds (N3−C28 = 1.406(3) Å and N4−C27 = 1.410(3) Å).[27]

A significant fold angle of approximately 55° exists between the planes defined by N4−C27−C28−N3 and N4−Zr1−N3. Fold angles of this size are commonly seen for complexes of this type. One related example is a bis(guanidinate) enediamido complex, which has a fold angle of 44.8°.[8] The deviation from planarity has been rationalized by the need to relieve steric interactions, as well as the additional electronic stabilization offered by the η^4-interaction with the metal center.[8,28b,d,29] While the Zr1−C27 and Zr1−C28 bond distances (2.560(2) and 2.548(2) Å, respectively) lie outside the range generally observed for Zr−C σ-bonds, they are similar to the distances observed in Cp complexes of Zr (average Zr−η^5-C_5H_5 distances are ~2.48−2.55 Å).[30]

Although it would be desirable to couple different isocyanide units to generate novel diamido ligands, the high reactivity of **4** results in rapid insertion of two equivalents of isocyanide per zirconium center, even with strict 1:1 stoichiometry. The rapid insertion of two equivalents of isocyanide into Zr−C bonds in the presence of only one equivalent of isocyanide is not generally seen. In most cases, insertion of a single isocyanide results in stable mixed alkyl η^2-iminoacyl complexes.[24] However, the observed reactivity reported here is consistent with both the greater steric access and enhanced electrophilic character of zirconium afforded by the amidate ligands in **4**.

With the knowledge that literature precedent for C−C coupling of iminoacyls is favored with electron-withdrawing groups, such as 2,6-dimethylphenyl, and disfavored with electron-donating groups, the possibility of divergent behavior was investigated by studying the insertion of *tert*-butyl isocyanide.[24,29] Upon addition of two equivalents of $^tBuN{\equiv}C$ to **4**, the solution immediately deepens in color from pale yellow to an intense golden yellow. The ^1H NMR spectrum of the insertion product **10** is consistent with a C_2 symmetric complex: there is one signal for the aryl methyl groups and two signals for the *tert*-butyl groups of the amidate ligands and inserted isocyanide units. Splitting of the signal for the benzylic protons in **10** into two canted doublets is suggestive of isocyanide insertion; however, the chemical shift of these signals is shifted far downfield at δ 5.84 and 7.28. These chemical shifts instead suggest the presence of vinyl amido ligands as shown in eq 6.[6c,24,31] The $^3J_{HH}$ coupling constants of 14 Hz for these signals indicate a *trans* geometry about the double bond.[27]

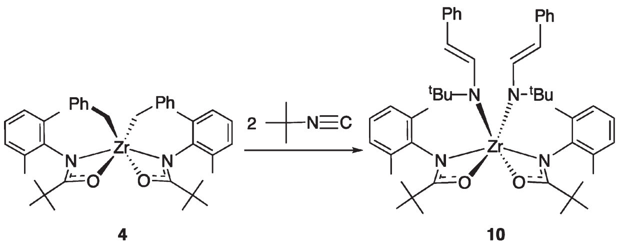

(6)

Vinylamido insertion products such as $[^{DMP}(NO)^{tBu}]_2$-$Zr(N(^tBu)CH{=}CHPh)_2$ (**10**) have been reported in the literature, but are relatively rare for group 4 metals.[6e,31b,c] Rothwell and co-workers reported a vinylamido hafnocene complex that resulted from the insertion of 2,6-dimethylphenyl isocyanide into the Hf−C bonds of $Cp_2Hf(CH_2\text{-py-6-}Me)_2$.[31b] In that case, the solid-state molecular structure of the insertion product clearly established the *trans* geometry of the vinyl group, and doublets for the *trans* vinyl protons were observed in the ^1H NMR spectrum at δ 4.6−4.8 and 8.5−9.5, with $^3J_{HH}$ coupling constants of 12−13 Hz.[31b]

---

(27) Smith, M. B.; March, J. *March's Advanced Organic Chemistry: Reactions, Mechanisms, and Structure*, 5th ed.; Wiley: Toronto, 2001.

(28) (a) McMullen, A. K.; Rothwell, I. P.; Huffman, J. C. *J. Am. Chem. Soc.* **1985**, *107*, 1072–1073. (b) Chamberlain, L. R.; Durfee, L. D.; Fanwick, P. E.; Kobriger, L. M.; Latesky, S. L.; McMullen, A. K.; Steffey, B. D.; Rothwell, I. P.; Foltin, K.; Huffman, J. C. *J. Am. Chem. Soc.* **1987**, *109*, 6068–6076. (c) Ramos, C.; Royo, P.; Lanfranchi, M.; Pellinghelli, M. A.; Tiripicchio, A. *Eur. J. Inorg. Chem.* **2005**, 3962–3970. (d) Giannini, L.; Caselli, A.; Solari, E.; Floriani, C.; Chiesi-Villa, A.; Rizzoli, C.; Re, N.; Sgamellotti, A. *J. Am. Chem. Soc.* **1997**, *119*, 9709–9719.

(29) Durfee, L. D.; McMullen, A. K.; Rothwell, I. P. *J. Am. Chem. Soc.* **1988**, *110*, 1463–1467.

(30) Barger, P. T.; Santarsiero, B. D.; Armantrout, J.; Bercaw, J. E. *J. Am. Chem. Soc.* **1984**, *106*, 5178–5186.

(31) (a) Beshouri, S. M.; Chebi, D. E.; Fanwick, P. E.; Rothwell, I. P.; Huffman, J. C. *Organometallics* **1990**, *9*, 2375–2385. (b) Beshouri, S. M.; Fanwick, P. E.; Rothwell, I. P.; Huffman, J. C. *Organometallics* **1987**, *6*, 891–893. (c) Lee, L.; Berg, D. J.; Bushnell, G. W. *Organometallics* **1997**, *16*, 2556–2561.

A related bis(guanidinate) dibenzyl Zr complex was shown to insert two equivalents of xylyl isocyanide, resulting in the formation of a bis(guanidinate) bis(vinylamido) product, analogous to **10**.[6e] The close similarity in the diagnostic NMR spectroscopic signals between these complexes and those of **10** lend further support to the proposed structure in eq 6.[6e,31b] In addition to the ^{1}H NMR spectroscopic data, ^{13}C NMR spectroscopy supports the presence of a vinyl group, with signals at δ 106.2 and 134.4, consistent with sp^2-hybridized carbon centers. It has also been reported that vinylamido ligands can be accessed through primary amine additions to alkynes coordinated to tungsten pyrazolyl borate complexes.[32] In these cases, the ^{1}H NMR spectroscopic data are very similar to those obtained for **10**, supporting the formulation in eq 6. Finally, mass spectrometry data of **10**, which is isolated as a bright yellow powder in 86% yield, confirm the insertion of two equivalents of ^{t}BuN≡C into **4**, to give a parent ion of m/z = 846. While X-ray crystallographic verification of this structure was not possible, the data presented are strongly supportive of the designation given in eq 6.

The isomerization of η^2-iminoacyl groups to vinylamides can be rationalized by a 1,2-hydrogen migration.[31a,b] The difference in reactivity seen for insertion of ^{t}BuN≡C versus 2,6-$Me_2C_6H_3N$≡C can be explained by two factors. First, the presence of the electron-donating *tert*-butyl group increases the energy of the π^*_{CN} orbital, making the C−C coupling of the η^2-iminoacyl groups much less favorable.[24] Second, steric bulk has been noted as a factor that can reduce 1,2-hydrogen migration in Cp complexes of Hf, where the insertion of 2,6-$Me_2C_6H_3N$≡C into the α-phenyl-substituted pyridyl benzyl complex $Cp_2Hf(CHPh\text{-}py\text{-}6\text{-}Me)_2$ results in the generation of the bis(η^2-iminoacyl) complex, and 1,2-hydrogen atom migration to the bis(vinylamido) complex cannot be induced.[31a] This is in contrast to the less sterically demanding pyridyl benzyl system $Cp_2Hf(CH_2\text{-}py\text{-}6\text{-}Me)_2$, which isomerizes to a vinylamido species upon insertion of 2,6-dimethylphenyl isocyanide.[31a] It is possible that the steric bulk of the amidate ligands in **4** prevents this rearrangement from occurring with 2,6-$Me_2C_6H_3N$≡C. However, the ^{t}BuN≡C group is less bulky by comparison and can rearrange to form the bis(vinylamido) complex **10**. While observation of the expected intermediate η^2-iminoacyl species was not possible for this reaction with **4**, an NMR tube scale reaction of Hf complex **1** with two equivalents of ^{t}BuN≡C resulted in the formation of the η^2-iminoacyl complex $[^{DMP}(NO)^{Ph}]_2Hf(\eta^2\text{-}{}^tBuN{=}CCH_2Ph)_2$ (**11**), as evidenced by ^{1}H NMR spectroscopic data, with diastereotopic benzylic resonances at δ 2.88 and 3.68. When the NMR tube is heated to 80 °C over 24 h, the solution changes color from yellow-orange to emerald green, showing diagnostic resonances at δ 6.02 and 7.74 for the *trans* vinyl group, indicating formation of the bis(vinylamido) complex $[^{DMP}(NO)^{Ph}]_2Hf(N(^tBu)CH{=}CHPh)_2$ (**12**). Unfortunately, there are also other side products observed in the reaction mixture, as evidenced by a number of other signals in the ^{1}H NMR spectrum.

Summary and Conclusions

In summary, amidate-supported zirconium and hafnium dibenzyl species can be reliably accessed in high yields through protonolysis of tetrabenzyl zirconium and hafnium starting materials with organic amide proligands. Both bidentate and tetradentate amidate ligands are successful at stabilizing these complexes. The zirconium complex **4** was less stable to heat and light than the previously reported hafnium complex **1** and exhibited intermediate η^1/η^2-hapticity of the benzyl ligands in the solid state, while behaving as an η^1-benzyl species in solution. Seven-coordinate species can be observed for both bidentate and tetradentate amidate-supported dibenzyl complexes, consistent with the reduced steric encumbrance of this asymmetric ligand set in comparison with related amidinate and guanidinate systems. Migratory insertion of aryl isocyanides was observed for **4**, resulting in the η^2-iminoacyl complex **8**, which can undergo thermal coupling to form enediamido complex **9**. Insertion of ^{t}BuN≡C resulted in the formation of a vinylamido complex, **10**, which is presumably generated from a transient η^2-iminoacyl intermediate via a 1,2-hydrogen migration. The inability to controllably insert one equivalent of isocyanide is indicative of the extremely electrophilic nature of **4**. All of the fundamental organometallic chemistry reported here is consistent with the unique coordination environment supported by the ionic character of the amidate bonding interactions in this family of complexes.[12]

Experimental Section

Except where stated otherwise, all manipulations were performed under an inert atmosphere of dry, oxygen-free dinitrogen using either standard Schlenk or drybox techniques. Anhydrous hexanes and toluene were purchased from Aldrich, sparged with dry, degassed dinitrogen, and passed through a column of activated alumina and Ridox (or Q-5) catalyst prior to use. Anhydrous benzene, diethyl ether, tetrahydrofuran, and pentane were purchased from Aldrich, sparged with dry, degassed dinitrogen, and purified by passage through an Innovative Technologies SPS-PureSolv-400-4 apparatus.

Deuterated NMR solvents were purchased from Cambridge Isotopes Ltd. Deuterated benzene (C_6D_6) and deuterated toluene (C_7D_8) were degassed by successive freeze−pump−thaw cycles and stored overnight over activated 4 Å molecular sieves under an atmosphere of dry dinitrogen prior to use. Deuterated chloroform ($CDCl_3$) was stored in a darkened flask over activated 4 Å molecular sieves prior to use with organic molecules. ^{1}H, ^{13}C, and two-dimensional spectra were collected on three different Bruker instruments: AV-300 with a 5 mm BBI probe operating at 300.0 MHz for ^{1}H NMR spectroscopy; AV-400 with a 5 mm inverse BBI probe operating at 400.0 MHz for ^{1}H NMR spectroscopy; AV-400 with a 5 mm BBI probe operating at 400.0 MHz for ^{1}H NMR spectroscopy. All three instruments were capable of variable-temperature experiments, ranging between −150 and +180 °C. ^{1}H NMR spectra were referenced to residual protons in deuterated solvents as follows: C_6D_5H (δ 7.15), C_7D_7H (δ 2.09), $CHCl_3$ (δ 7.24) with respect to TMS (δ 0.00). ^{13}C NMR spectra were referenced to δ 128.39 in deuterated benzene or δ 77.44 in deuterated chloroform with respect to TMS (δ 0.00).

Mass spectra were either collected on an Agilent Technologies GCMS equipped with a 6890N GC column and a 5793 mass selective detector operating with an electron impact source and quadrupolar detector or were collected by Mr. M. Lapawa at the University of British Columbia, Department of Chemistry (EIMS on a Kratos MS 50 using a 70 eV electron impact source, unless otherwise stated). Assigned mass clusters for specific ions in the mass spectra show the appropriate isotopic patterns as calculated for the atomic composition of the species. Elemental analyses were performed by Mr. M. Lakha at the University of

---

[32] Feng, S. G.; White, P. S.; Templeton, J. L. *Organometallics* **1995**, *14*, 5184–5192.

British Columbia, Department of Chemistry. Due to the air and moisture sensitivity of the metal complexes analyzed, these compounds were handled using glovebox or glovebag techniques during analysis. In this class of complexes satisfactory carbon analyses were problematic and repeated attempts typically resulted in satisfactory H and N analyses but low C. We suggest this may be due to incomplete combustion through carbide formation. To further support the characterization data presented in the Experimental Section, ^{1}H and ^{13}C NMR spectral data are included in the Supporting Information.

Crystallographic measurements were made on either Rigaku ADSC, Rigaku AFC7, or Bruker X8 Apex CCD area detectors with graphite-monochromated Mo Kα radiation. The data were processed[33] and corrected for Lorentz and polarization effects. The structures were solved by direct methods[34] and expanded using Fourier techniques.[35] All non-hydrogen atoms were refined with anisotropic thermal parameters. Neutral atom scattering factors and anomalous dispersion corrections were taken from the International Tables for X-ray Crystallography.[36a] All structures are visualized as ORTEP-3 depictions.[37]

The following reagents were purchased from Aldrich and purified by distillation: 2,6-dimethylaniline; $H_2NCH_2CMe_2CH_2NH_2$; benzoyl chloride; trimethylacetyl chloride; triethylamine; 1-adamantoyl chloride; tertbutylisocyanide. Benzyl magnesium chloride was purchased from Aldrich and used as received. $ZrCl_4$, $HfCl_4$, and 2,6-dimethylphenylisocyanide were purchased from Strem Chemicals and used without further purification. Compounds $Zr(CH_2Ph)_4$,[13] $Hf(CH_2Ph)_4$,[13] $[^{DMP}(NO)^{Ph}]H$,[14] $[^{DMP}(NO)^{Ph}]_2Hf(CH_2Ph)_2(THF)$ (**1**),[14] and $[^{DMP}(NO)^{tBu}]H$ (**3**)[11] were prepared via literature methods.

Synthesis of $[^{DMP}(NO)^{Ph}]_2Hf(CH_2Ph)_2$ (2). This complex was communicated previously, but full synthetic details and characterization data are presented here.[14] In a foil-wrapped Schlenk flask, 0.93 g (1.7 mmol) of $Hf(CH_2Ph)_4$ and 0.77 g (3.4 mmol) of $[^{DMP}(NO)^{Ph}]H$ were combined. To this mixture of solids was added approximately 75 mL of toluene at −78 °C via cannula. The reaction mixture was allowed to warm to room temperature while stirring for approximately 4 h. Excess toluene was removed, resulting in the isolation of a bright yellow solid residue. The crude product was dissolved in approximately 25 mL of hexanes at room temperature and concentrated until a yellow powder precipitated out of solution. This powder was isolated in 62% yield (0.86 g) by filtration through a fritted disk and dried *in vacuo*. ^{1}H NMR (C_6D_6, 25 °C, 300 MHz): δ 2.10 (s, 12H, $Ph(CH_3)_2$), 2.30 (s, 4H, $Hf(CH_2Ph)_2$), 6.78−6.94 (m, 14H total, Ar-*H*), 7.10−7.24 (m, 8H total, Ar-*H*), 7.61 (d, 4H, $^3J_{HH}$ = 7 Hz, Ar-*H*). $^{13}C\{^1H\}$ NMR (C_6D_6, 25 °C, 75 MHz): δ 19.0, 82.9, 122.1, 126.4, 129.0, 128.7, 129.3, 129.5, 130.1, 132.3, 132.7, 133.5, 142.5, 144.7, 179.6. EIMS (*m*/*z*): 719 ($[M^+] - CH_2Ph$), 627 ($[M^+] - 2\,CH_2Ph$). Anal. Calcd for $C_{44}H_{42}N_2O_2Hf$ (%): C, 65.30; H, 5.23; N, 3.46. Found: C, 64.41; H, 5.36; N, 3.81.

Synthesis of $[^{DMP}(NO)^{tBu}]_2Zr(CH_2Ph)_2$ (4). In a foil-wrapped 250 mL round-bottomed Schlenk flask equipped with a stir bar, 0.90 g (4.4 mmol) of $[^{DMP}(NO)^{tBu}]H$ (**3**) was combined with 1.00 g (2.2 mmol) of $Zr(CH_2Ph)_4$. To this flask was added 75 mL of toluene, which had been cooled to −78 °C. The reaction mixture was then stirred for 3.5 h while allowing to warm to ~10 °C. Given the thermal and photosensitivity of $Zr(CH_2Ph)_4$, care was taken to ensure reaction occurred in the absence of ambient light, and the reaction was not allowed to exceed 10 °C. The clear bright yellow solution was then concentrated to dryness *in vacuo* to give a bright yellow solid residue. The crude material was dissolved in 30 mL of pentane and filtered through Celite to remove impurities. The pentane solution was concentrated to approximately 10 mL and cooled to −37 °C. The yellow precipitate was isolated in 57% yield (0.85 g) by filtration and dried *in vacuo*. Successive concentration/filtration cycles allow access to > 80% yield of pure **4**. Single crystals suitable for X-ray crystallographic analysis were grown in the dark from a saturated pentane solution at −37 °C. ^{1}H NMR (C_6D_6, 25 °C, 300 MHz): δ 0.91 (s, 18H, $C(CH_3)_3$), 2.05 (s, 12H, $Ph(CH_3)_2$), 2.24 (s, 4H, $Zr(CH_2Ph)_2$), 6.86−6.89 (m, 8H, Ar-*H*), 7.11−7.15 (m, 8H, Ar-*H*). $^{13}C\{^1H\}$ NMR (C_6D_6, 25 °C, 75 MHz): δ 19.4, 27.5, 41.2, 75.8, 123.1, 125.5, 128.6, 129.4, 129.9, 132.1, 142.9, 143.2, 190.7. EIMS (*m*/*z*): 589 ($[M^+] - CH_2Ph$), 497 ($[M^+] - 2\,CH_2Ph$). Anal. Calcd for $C_{40}H_{50}N_2O_2Zr$ (%): C, 70.44; H, 7.39; N, 4.11. Found: C, 69.71; H, 7.60; N, 4.67.

Synthesis of $^{Ad}[O_2N_2]H_2$ (5). A solution of 1,3-diamino-2,2-dimethylpropane (2.4 mL, 20.1 mmol) and triethylamine (5.6 mL, 40.3 mmol) in 100 mL of CH_2Cl_2 was cooled to −78 °C prior to dropwise addition of a CH_2Cl_2 solution of 1-adamantane carbonyl chloride (7.98 g, 40.3 mmol). The clear, colorless solution was allowed to warm to room temperature while stirring overnight. The cloudy white suspension was then extracted with three portions of 1 M HCl (3 × 25 mL) until the aqueous washings were acidic. The organic fraction was then extracted with a single 25 mL portion of 1 M NaOH. Finally, the organic fraction was washed with 25 mL of brine, and the organic fraction was dried over anhydrous $MgSO_4$. Gravity filtration of the solution to remove $MgSO_4$ was performed, and excess CH_2Cl_2 was removed by rotary evaporation to give a white powder. The product was purified by recrystallization from a supersaturated toluene solution that was cooled to −15 °C. A white solid was isolated by filtration, ground with a mortar and pestle to a fine white powder, and dried while heating to 120 °C under vacuum overnight in a Schlenk flask to remove air and moisture. Due to the increased ability of **5** to hydrogen bond with water, the elevated temperature was used to remove traces of moisture. The purified product was isolated in 67% yield (5.75 g). ^{1}H NMR ($CDCl_3$, 25 °C, 300 MHz): δ 0.80 (s, 6H, $HNCH_2C(CH_3)_2CH_2NH$), 1.70 (br, 12H, Ad-$(CH(CH_2)CH)_3$), 1.86 (d, 12H, $^3J_{HH}$ = 3 Hz, Ad-$C(CH_2)_3$), 2.02 (br, 6H, Ad-$(CH)_3$), 2.91 (d, 4H, $^3J_{HH}$ = 7 Hz, $HNCH_2C(CH_3)_2CH_2NH$), 6.54 (t, 2H, $^3J_{HH}$ = 6 Hz, N*H*). $^{13}C\{^1H\}$ NMR ($CDCl_3$, 25 °C, 75 MHz): δ 23.5, 28.2, 36.5, 39.3, 40.8, 44.9, 178.7 (no signal observed for quaternary C of adamantyl group). CIMS (*m*/*z*): 427 ($[M + 1^+]$). Anal. Calcd for $C_{27}H_{42}N_2O_2$ (%): C, 76.01; H, 9.92; N, 6.57. Found: C, 75.69; H, 9.96; N, 6.70.

Synthesis of $^{Ad}[O_2N_2]Zr(CH_2Ph)_2(THF)$ (6). A foil-wrapped 250 mL round-bottomed Schlenk flask equipped with a stir bar was loaded with 0.75 g (1.7 mmol) of $Zr(CH_2Ph)_4$. To this flask was added 50 mL of THF via cannula, and the resulting solution was cooled to −78 °C. Using a solid addition funnel, 0.70 g (1.7 mmol) of **5** was added to the THF solution of $Zr(CH_2Ph)_4$ over a period of 5 min. The cloudy yellow reaction mixture was then stirred while warming to 0 °C over the course of 4 h. The clear, bright yellow-orange solution was concentrated to dryness *in vacuo* to give a bright yellow solid residue, while ensuring that the reaction temperature did not exceed ~10 °C. The crude material was washed with 25 mL of pentane and dried under vacuum to give a bright yellow powder in 73% yield (0.92 g). Single crystals suitable for X-ray crystallographic analysis were grown in the dark from a saturated hexanes solution at −37 °C. ^{1}H NMR (C_6D_6, 25 °C, 400 MHz): δ 0.72 (s, 6H, $C(CH_3)_2$), 1.38 (m, 4H, $O(CH_2CH_2)_2$), 1.61 (br, 12H, Ad-$(CH(CH_2)CH)_3$), 1.90 (br, 6H, Ad-$(CH)_3$), 2.04 (br, 12H, Ad-$C(CH_2)_3$), 2.25 (s, 4H, $Zr(CH_2Ph)_2$), 3.08 (s, 4H, $NCH_2C(CH_3)_2CH_2N$), 3.66 (m, 4H,

---

[33] *teXan*; Molecular Structure Corp.: The Woodlands, TX, 1996.

[34] Altomane, A.; Burla, M. C.; Cammali, G.; Cascarano, M.; Giacovazzo, C.; Gagliardi, A.; Moliterni, A. G. G.; Polidoi, G.; Spagna, A. *SIR-97*; CNR-IRMEC: Bari, Italy, 1999.

[35] Beurkens, P. T.; Admiraal, G.; Baurskens, G.; Bosman, W. P.; de Gelder, R.; Israel, R.; Smits, J. M. M. *DIRDIF94*; University of Njmegen: Njmegen, The Netherlands, 1994.

[36] (a) International Union of Crystallography. *International Tables for X-ray Crystallography*; Kynoch Press: Birmingham, UK, 1974. (b) International Union of Crystallography. *International Tables for X-ray Crystallography*; Kluwer Academic: Boston, MA, 1992.

[37] Farrugia, L. J. *J. Appl. Crystallogr.* **1997**, *30*, 565.

$\mathrm{O(C}H_2\mathrm{CH_2)_2)}$, 6.86 (m, 2H, Ar-$H$), 7.19−7.24 (m, 8H, Ar-$H$). $^{13}\mathrm{C}\{^1\mathrm{H}\}$ NMR ($\mathrm{C_6D_6}$, 25 °C, 100 MHz): δ 24.9, 26.0, 28.9, 35.8, 37.2, 38.5, 43.0, 56.3, 62.4, 68.8, 120.2, 127.9, 128.5, 148.2, 192.3. EIMS (m/z): 605 ($[\mathrm{M}^+]$ − THF − $\mathrm{CH_2Ph}$). Anal. Calcd for $\mathrm{C_{45}H_{62}N_2O_3Zr}$ (%): C, 70.17; H, 8.11; N, 3.64. Found: C, 65.01; H, 7.99; N, 4.14.

Synthesis of $^{\mathrm{Ad}}[\mathrm{O_2N_2}]\mathrm{Hf(CH_2Ph)_2(THF)}$ (7). A foil-wrapped 250 mL round-bottomed Schlenk flask equipped with a stir bar was loaded with 3.00 g (5.5 mmol) of $\mathrm{Hf(CH_2Ph)_4}$. To this flask was added 100 mL of THF via cannula, and the resulting solution was cooled to −78 °C. Using a solid addition funnel, 2.36 g (5.5 mmol) of **5** was added to the THF solution of $\mathrm{Hf(CH_2Ph)_4}$ over a period of 5 min. The cloudy yellow reaction mixture was then stirred while warming to room temperature overnight. The clear yellow solution was then concentrated to dryness *in vacuo* to give a light yellow solid residue. The crude material was triturated with ~30 mL of pentane and filtered over a fritted disk to give 2.75 g (58% yield) of **7** as a pale yellow powder. The pentane washings were concentrated until product began to precipitate. After cooling to aid precipitation, an additional 0.50 g (12% yield) of **7** was isolated by filtration, resulting in an overall isolated yield of 70%. Single crystals suitable for X-ray crystallographic analysis were grown in the dark from a saturated hexanes solution at −37 °C. ^{1}H NMR ($\mathrm{C_6D_6}$, 25 °C, 400 MHz): δ 0.83 (s, 6H, $\mathrm{C(C}H_3\mathrm{)_2}$), 1.33 (m, 4H, $\mathrm{O(CH_2C}H_2\mathrm{)_2}$), 1.66 (br, 12H, Ad-($\mathrm{CH(C}H_2\mathrm{)CH)_3}$), 1.73 (s, 4H, $\mathrm{Hf(C}H_2\mathrm{Ph)_2}$), 1.95 (br, 6H, Ad-($\mathrm{C}H\mathrm{)_3}$), 2.09 (br, 12H, Ad-$\mathrm{C(C}H_2\mathrm{)_3}$), 3.19 (s, 4H, $\mathrm{NC}H_2\mathrm{C(CH_3)_2C}H_2\mathrm{N}$), 3.99 (m, 4H, $\mathrm{O(C}H_2\mathrm{CH_2)_2}$), 6.76 (m, 2H, Ar-$H$), 7.04 (d, 4H, $^3J_{\mathrm{HH}}$ = 8 Hz, Ar-H), 7.19 (m, 4H, Ar-H). $^{13}\mathrm{C}\{^1\mathrm{H}\}$ NMR ($\mathrm{C_6D_6}$, 25 °C, 75 MHz): δ 24.9, 25.0, 28.2, 35.8, 36.5, 37.8, 42.8, 55.3, 57.3, 70.0, 117.9, 125.4, 127.4, 153.9, 190.9. EIMS (m/z): 695 ($[\mathrm{M}^+]$ − THF − $\mathrm{CH_2Ph}$). Anal. Calcd for $\mathrm{C_{45}H_{62}N_2O_3Hf}$ (%): C, 63.03; H, 7.29; N, 3.27. Found: C, 61.96; H, 7.64; N, 3.50.

Synthesis of $[^{\mathrm{DMP}}(\mathrm{NO})^{\mathrm{tBu}}]_2\mathrm{Zr}(\eta^2\text{-}\mathrm{ArN{=}CCH_2Ph})_2$ (Ar = 2,6-$\mathrm{Me_2C_6H_3}$) (8). In a 50 mL Schlenk flask, 0.15 g (0.2 mmol) of **4** was dissolved in approximately 5 mL of toluene at room temperature. To this solution was added 0.058 g (0.4 mmol) of 2,6-$\mathrm{Me_2C_6H_3N{\equiv}C}$ dissolved in 5 mL of toluene. The bright yellow solution was stirred at room temperature and became colorless within minutes. Excess toluene was removed *in vacuo* to give a white residue. This material was triturated with 5 mL of pentane, and the insoluble white powder was isolated by filtration in 52% yield (0.108 g). Higher yields are possible, but due to static electricity, the product sticks to glass very well, and small-scale reactions suffer from this. Single crystals were grown from a saturated pentane solution at −37 °C. ^{1}H NMR ($\mathrm{C_6D_6}$, 25 °C, 300 MHz): δ 0.95 (s, 6H, $\mathrm{Ph(C}H_3\mathrm{)_2}$), 1.11 (s, 18H, $\mathrm{C(C}H_3\mathrm{)_3}$), 1.92 (s, 6H, $\mathrm{Ph(C}H_3\mathrm{)_2}$), 2.12 (s, 6H, $\mathrm{Ph(C}H_3\mathrm{)_2}$), 2.62 (s, 6H, Ph-$\mathrm{(C}H_3\mathrm{)_2}$), 3.35 (d, 2H, $^2J_{\mathrm{HH}}$ = 12 Hz, $\mathrm{C}H_2\mathrm{Ph}$), 3.59 (d, 2H, $^2J_{\mathrm{HH}}$ = 12 Hz, $\mathrm{C}H_2\mathrm{Ph}$), 6.19 (d, 4H, $^3J_{\mathrm{HH}}$ = 7 Hz, Ar-H), 6.83−7.09 (m, 18H, Ar-H). $^{13}\mathrm{C}\{^1\mathrm{H}\}$ NMR ($\mathrm{C_6D_6}$, 25 °C, 75 MHz): δ 18.2, 19.1, 19.4, 20.6, 28.5, 41.3, 44.3, 125.7, 125.8, 126.6, 129.0, 130.0, 130.2, 130.8, 133.5, 133.9, 135.8, 147.8, 149.1, 187.3, 250.6. EIMS (m/z): 942 ($[\mathrm{M}^+]$), 720 ($[\mathrm{M}^+]$ − $\mathrm{PhCH_2C{=}N(2,6\text{-}Me_2C_6H_3)}$). Anal. Calcd for $\mathrm{C_{58}H_{68}N_4O_2Zr_1}$ (%): C, 73.76; H, 7.26; N, 5.93. Found: C, 70.62; H, 7.25; N, 5.63.

Synthesis of $[^{\mathrm{DMP}}(\mathrm{NO})^{\mathrm{tBu}}]_2\mathrm{Zr}(\eta^4\text{-}\mathrm{ArNC(CH_2Ph){=}C(CH_2Ph)\text{-}NAr})$ (Ar = 2,6-$\mathrm{Me_2C_6H_3}$) (9). In a 100 mL Schlenk flask, 0.360 g (0.5 mmol) of **4** and 0.139 g (1.0 mmol) of 2,6-$\mathrm{Me_2C_6H_3N{\equiv}C}$ were dissolved in approximately 35 mL of toluene at room temperature. The bright yellow solution was stirred and heated to 110 °C overnight, resulting in a yellow-orange solution. Excess toluene was removed *in vacuo* to give a yellow-orange solid. This material was dissolved in 10 mL of pentane and filtered through Celite to remove **8**. Excess pentane was removed *in vacuo*, resulting in 81% yield (0.403 g) of **9** as a yellow-orange solid. This complex can also be synthesized by heating **8** to 110 °C overnight. Single crystals for X-ray analysis were grown from a saturated toluene solution at room temperature. ^{1}H NMR ($\mathrm{C_6D_6}$, 25 °C, 400 MHz): δ 0.82 (s, 18H, $\mathrm{C(C}H_3\mathrm{)_3}$), 1.95 (s, 12H, $\mathrm{Ph(C}H_3\mathrm{)_2}$), 2.19 (s, 12H, $\mathrm{Ph(C}H_3\mathrm{)_2}$), 3.99 (s, 4H, $\mathrm{C}H_2\mathrm{Ph}$), 6.65−7.08 (m, 22H, Ar-H). $^{13}\mathrm{C}\{^1\mathrm{H}\}$ NMR ($\mathrm{C_6D_6}$, 25 °C, 100 MHz): δ 20.2, 21.2, 28.1, 37.8, 41.4, 115.6, 124.1, 124.8, 126.3, 128.0, 128.3, 128.6, 130.5, 132.1, 133.3, 140.4, 143.9, 147.3, 187.6.

Synthesis of $[^{\mathrm{DMP}}(\mathrm{NO})^{\mathrm{tBu}}]_2\mathrm{Zr}(\mathrm{N^tBuCH{=}CHPh})_2$ (10). In a 100 mL Schlenk flask, 0.360 g (0.5 mmol) of **4** was dissolved in approximately 30 mL of toluene at room temperature. To this solution was added 0.088 g (1.0 mmol) of $^{\mathrm{t}}\mathrm{BuN{\equiv}C}$ dissolved in 5 mL of toluene at room temperature. The solution immediately became an intense yellow color. Excess toluene was removed *in vacuo* to give a vibrant yellow solid. This material was triturated with 10 mL of pentane and isolated by filtration in 86% yield (0.385 g). ^{1}H NMR ($\mathrm{C_6D_6}$, 25 °C, 300 MHz): δ 1.02 (s, 18H, $\mathrm{O{=}CC(C}H_3\mathrm{)_3}$), 1.35 (s, 18H, $\mathrm{NC(C}H_3\mathrm{)_3}$), 2.31 (s, 12H, $\mathrm{Ph(C}H_3\mathrm{)_2}$), 5.84 (d, 2H, $^3J_{\mathrm{HH}}$ = 14 Hz, $\mathrm{NC}H\mathrm{{=}CHPh}$), 6.91−7.12 (m, 16H, Ar-H), 7.28 (d, 2H, $^3J_{\mathrm{HH}}$ = 14 Hz, $\mathrm{NCH{=}C}H\mathrm{Ph}$). $^{13}\mathrm{C}\{^1\mathrm{H}\}$ NMR ($\mathrm{C_6D_6}$, 25 °C, 75 MHz): δ 20.9, 28.3, 30.4, 41.3, 58.4, 106.2, 124.7, 125.2, 125.9, 128.1, 129.0, 132.1, 134.4, 139.5, 144.7 (no signal seen for C=O). EIMS (m/z): 846 ($[\mathrm{M}^+]$). Anal. Calcd for $\mathrm{C_{50}H_{68}N_4O_2Zr_1}$ (%): C, 70.79; H, 8.08; N, 6.60. Found: C, 69.42; H, 7.73; N, 6.16.

NMR Tube Reaction of 1 and $^{\mathrm{t}}\mathrm{BuN{\equiv}C}$ to Generate $[^{\mathrm{DMP}}(\mathrm{NO})^{\mathrm{Ph}}]_2\mathrm{Hf}(\eta^2\text{-}^{\mathrm{t}}\mathrm{BuN{=}CCH_2Ph})_2$ (11) and $[^{\mathrm{DMP}}(\mathrm{NO})^{\mathrm{Ph}}]_2\text{-}\mathrm{Hf}(\mathrm{N^tBuCH{=}CHPh})_2$ (12). In a 20 mL scintillation vial, 0.100 g (0.1 mmol) of **1** was dissolved in approximately 0.5 mL of $\mathrm{C_6D_6}$ and transferred into a J-Young NMR tube. In another vial 0.019 g (0.2 mmol) of $^{\mathrm{t}}\mathrm{BuN{\equiv}C}$ was dissolved in approximately 0.5 mL of $\mathrm{C_6D_6}$ and added to the NMR tube. An immediate color change from orange to yellow-orange occurred upon mixing the two solutions. While the ^{1}H NMR spectrum was complicated and indicated a mixture of products, signals characteristic of an η^2-iminoacyl (**11**) were observed. ^{1}H NMR ($\mathrm{C_6D_6}$, 25 °C, 300 MHz): δ 2.88 (d, 2H, $^2J_{\mathrm{HH}}$ = 13 Hz, $^{\mathrm{t}}\mathrm{BuN{=}CC}H_2\mathrm{Ph}$), 3.68 (d, 2H, $^2J_{\mathrm{HH}}$ = 14 Hz, $^{\mathrm{t}}\mathrm{BuN{=}CC}H_2\mathrm{Ph}$). Heating the NMR tube to 80 °C for 24 h resulted in a gradual color change from yellow-orange to red-brown and finally to emerald green. Again, the ^{1}H NMR spectrum was complicated with signals for multiple products, and signals characteristic of a *trans* vinylamido complex (**12**) analogous to **10** were observed. ^{1}H NMR ($\mathrm{C_6D_6}$, 25 °C, 300 MHz): δ 6.02 (d, 2H, $^3J_{\mathrm{HH}}$ = 13 Hz, $^{\mathrm{t}}\mathrm{BuNC}H\mathrm{{=}CHPh}$), 7.74 (d, 2H, $^3J_{\mathrm{HH}}$ = 12 Hz, $^{\mathrm{t}}\mathrm{BuNCH{=}C}H\mathrm{Ph}$).

Acknowledgment. The authors wish to thank B. O. Patrick for assistance with X-ray crystallography, and UBC, CFI, BCKDF, and NSERC for financial support of this work. R.K.T. thanks NSERC for a postgraduate scholarship.

Supporting Information Available: Crystallographic information files (CIFs) of complexes **4**, **6**, **7**, **8**, and **9** are available, as well as selected NMR spectra for the complexes reported. This material is available free of charge via the Internet at http://pubs.acs.org.